

Development of a Simple Computer Code to Obtain Relevant Data on H₂ and CO Combustion in Severe Accidents and to Aid in PSA-2 Assessments

Fernando Robledo

Consejo de Seguridad Nuclear (CSN); Spain

Juan M. Martín-Valdepeñas

Consejo de Seguridad Nuclear (CSN); Spain

Miguel A. Jiménez

Consejo de Seguridad Nuclear (CSN); Spain

Francisco Martín-Fuertes

Polytechnic University of Madrid (UPM); Spain

1. Introduction

By following Consejo de Seguridad Nuclear (CSN) requirements, all of the Spanish NPP's performed plant specific PSA level 2 studies and implemented Severe Accident Management Guidelines during the first years of this century. CSN and contractors made an independent detailed review of these PSA level 2 studies (Khatib-Rahbar 1997 - 2002). This independent review included the performance of plant specific calculations by using the MELCOR code and some other stand-alone codes and the calculation of the fission product release frequencies for each plant. One of the aspects treated in detail by CSN evaluations was the calculation of the containment failure probability due to the burn of combustible gases generated during a severe accident. It was shown that it would be useful to have a fast running code with capability to provide the most relevant data concerning H₂ and CO combustion. Therefore, the Polytechnic University of Madrid (UPM) developed the CPPC code (Martín-Valdepeñas, 2004a) for the CSN. This stand-alone module makes fast calculations on maximum static pressures in the containment building generated from H₂ and CO combustion in severe accidents, considering well-mixed atmospheres and includes the most recent advances and developments in the field of H₂ and CO combustion. Code input is simple: mass of H₂ and CO, initial environmental conditions inside the containment before the combustion and simple geometric data, such as the volume of the building enclosing the combustible gases. The code calculates the containment temperature assuming steam saturated atmosphere and provides the following output:

- Combustion completeness (CC).
- Adiabatic and isochoric combustion pressure (p_{AICC}).
- Chapman-Jouguet pressure (p_{CJ}).
- Chapman-Jouguet reflected pressure (p_{CJrefl}).

When the combustion regime results in dynamic pressure loads, the CPPC code calculates the equivalent static pressure (effective pressure p_{eff}) by modeling the containment structure as a simple harmonic oscillator. Additionally, the code provides the atmosphere composition and indicates the combustion regime expected (non-flammable, SD: slow deflagration, FA: deflagration with flame acceleration, DDT: deflagration-to-detonation transition and DET: direct detonation) by applying the σ

and λ criteria developed by the Forschungszentrum Karlsruhe (FzK) and the Kurchatov Institute Moscow (KI).

This paper describes the main characteristics of this code, the code verification and validation process and outlines some of the main applications considered by the CSN as future activities.

2. Theoretical models and assumptions

Models implemented in the CPPC code are described in this section by following, as much as possible, the calculation sequence of the code.

2.1. Random sampling of the H₂ in-vessel release

The first step consists of performing a random sampling of the H₂ released mass during the in-vessel phase of the severe accident. The values are taken from the cumulative probability distribution of the H₂ release as results of the PSA-2 analysis for the plant. This sampling is applied only at the in-vessel phase of the analysis. At the ex-vessel phase the flammable gas releases are not usually expressed as probability distributions, but the code directly calculates pressures for each of the points (mass of H₂, CO and CO₂ released) included at the input file.

2.2. Partial pressure and temperature calculation from the initial conditions

Initial conditions for the calculations are the containment free volume and the containment pressure during the accident at the instant previous to the postulated combustion. Other data needed for the calculation (air and steam moles and atmosphere temperature) are calculated under the following assumptions, hence avoiding to perform full containment simulations for every sequence of the PSA-2 analysis:

- The containment atmosphere before the accident was at 1 bar, 49°C, 60% humidity.
- There were not any previous combustion at the containment.
- The containment gases are homogeneously mixed and are ideal gases.
- Steam-saturated atmosphere conditions at the instant previous to the postulated combustion.

Upon these hypothesis, atmosphere temperature (T_u) and steam and non-condensable gas partial pressures are calculated by calculating the saturation pressure from the expressions of the "TabAgua" program, developed by Centro Atómico de Bariloche (CAB, 1998).

2.3. Flammability limits

The combustion process occurs provided an ignition source and if the hydrogen/air/steam mixture composition lies within the flammability limits. Assessment of ignition sources is neglected in this analysis, because of the random feature of this process during an accidental sequence. Factors affecting flammability limits are:

- atmosphere composition,
- lean / rich hydrogen mixtures,
- flame propagation orientation and
- initial temperature conditions.

Even though flammability limits are not a property of the mixture, they are very useful for applications in engineering and safety studies, since they are indicative of the mixture ability to maintain the flame propagation after the energy release by and ignition source (Stamps, 1991). Several experimental programs evaluated these limits (Kumar, 1985) and (Marshal, 1986). After the review by (Stamps, 1991), flammability limits widen with the temperature. Moreover, buoyancy and diffusion processes make the limits depend on the orientation of the propagation front, especially for lean

mixtures. Finally, the steam concentration affects mainly at values around 50% vol., where the experimental results show the largest uncertainties. Lean mixture behaviour is governed by hydrogen concentration and, by contrast, rich mixtures are governed by air (oxygen) concentration.

The CPPC code makes use of an expression for the upward flammability limits (Marshal, 1986), corrected to account for the initial temperature of the mixture. Notice that the upward flammability limits have been only considered since they are meant to be the most favourable conditions for combustion. This expression depends on the hydrogen and steam molar fractions (X_{H_2} , X_{H_2O}) and temperature (T_u):

$$X_{H_2O} = a_f + b_f X_{H_2} + c_f e^{d_f X_{H_2} + b_f T_u} \quad (\text{Eq.2.1})$$

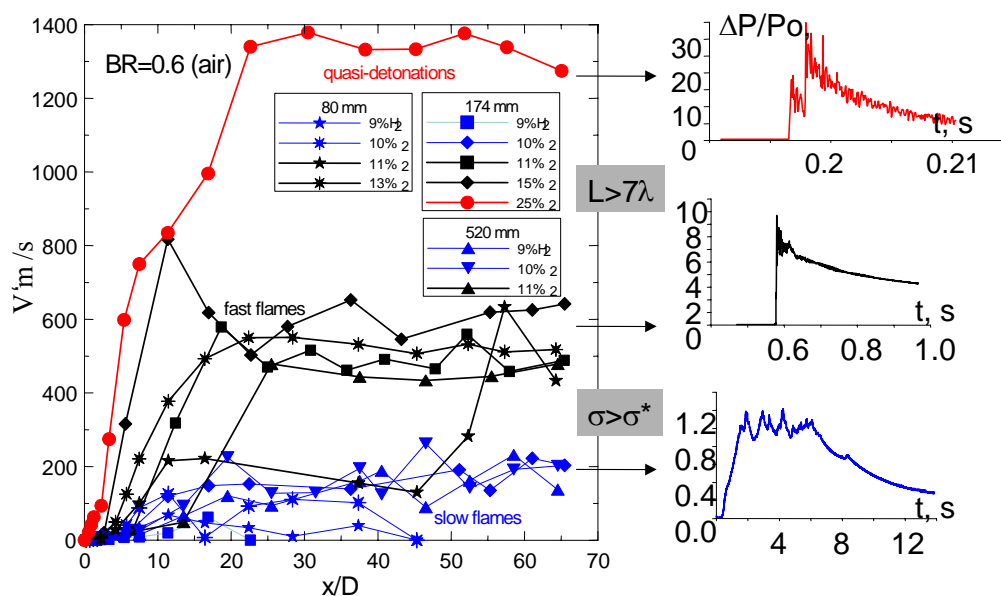
being a_f , b_f , c_f and d_f coefficients fitted experimentally (Martín-Valdepeñas, 2004b).

2.4. Combustion regimes

Different hydrogen combustion regimes could happen during a severe accident, because the hydrogen concentration could reach values up to some 20 % vol. with the steam concentration ranging between 20 and 70% vol. (CSNI, 2000). Moreover, mixing and distribution processes could drive to either well-mixed or inhomogeneous conditions (stratification, local accumulation, etc.). If an ignition source were present the hydrogen could burn in different conditions, depending on the mixture composition and the flow geometry. Combustion regime, from the point of view of nuclear safety, could be classified in the following categories (CSNI, 2000), (Dorofeev, 2001), (Kuznetsov, 2003):

- Slow deflagration (SD): flame speed is lower than the reactant sound velocity (>200 m/s) and the pressure increase is of the order of the initial one.
- Flame acceleration (FA): flame speed is higher than the reactant sound velocity, but lower than product sound velocity (>500 m/s) and the dynamic pressure increases some ten times the initial one.
- Deflagration-to-detonation transition (DDT): flame speed is higher than the product sound velocity (~1200m/s) and the dynamic pressure increases about thirty times the initial one.
- Direct detonation (DET): the flame speed is higher than the product sound velocity and the dynamic pressure increases about thirty times the initial one.

Figure 2.1. Hydrogen combustion regime: (left) flame speeds along the experimental facility and (right) dynamic combustion pressure, taken from (Kuznetsov, 2003).



The main difference between DDT and DET is the initiation mechanism: DDT is initiated by flame acceleration processes by turbulence effects of the obstacles on the flame front, DET needs higher hydrogen concentrations and ignition energies high enough (10 – 1000 kJ). Figure 2.1 shows flame speed and pressure typical of the different combustion regimes, as resulted from tests performed in experimental tubes of several sizes and blockage relations (BR) for lean hydrogen mixtures.

2.4.1. Slow deflagration (SD)

This regime is assessed by checking whether the inert gas concentration is lower than the value expressed by the (Eq.2.1) and the following criteria are not met.

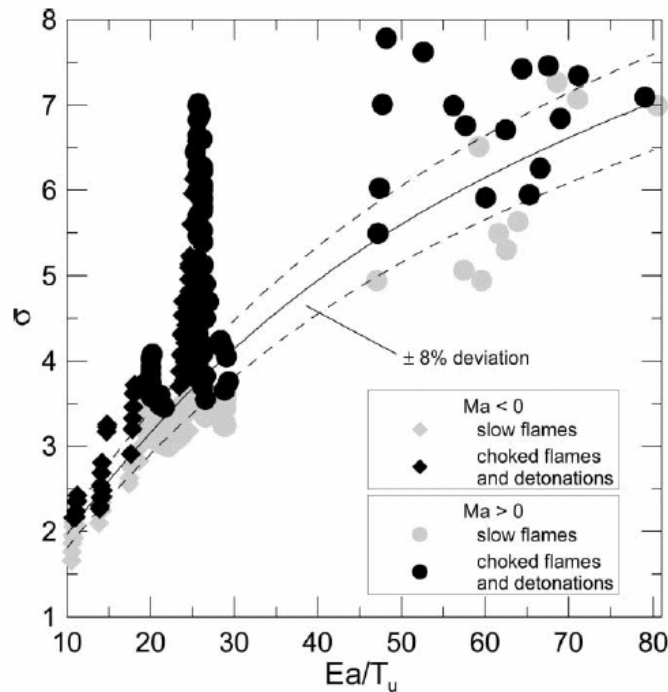
2.4.2. Flame acceleration (FA): the σ -criterion

FzK and KI (CSNI, 2000) have performed several experimental series (tubes from 0.08 to 2.25 m in diameter, several blockage ratios and mixture concentrations) and reviewed the experimental data of the literature. They concluded that the FA does not depend on geometrical scale and blockage conditions, but depends on the initial properties of the mixture (Breitung and Royl, 2000), if enough turbulence is developed. The best parameter correlating the FA occurrence is the expansion ratio, known as “ σ ” parameter:

$$\sigma = \frac{v_b}{v_u} = \frac{\rho_u}{\rho_b} \quad (\text{Eq.2.2})$$

i.e. the ratio between the specific volume of the burned (v_b) and unburned (v_u) mixtures. Burned mixture properties are calculated assuming the adiabatic isobaric complete combustion of ideal gases.

Figure 2.2. Combustion regime as function of expansion ratio and activation energy.



Dorofeev et al. (2001) demonstrated that there is a critical value (σ^*) separating the mixtures experiencing simple SD from the mixtures undergoing FA, Figure.2.2. This value depends on the Zeldovich number and the Lewis number, and has been fitted by a polynomial function:

$$\sigma^* = a_\sigma + b_\sigma \left(\frac{E_a}{T_u} \right)^{c_\sigma} \quad (\text{Eq.2.3})$$

being a_σ , b_σ and c_σ the correlation coefficients. The activation energy is calculated by a polynomial function of the equivalence ratio, fitted to experimental and thermodynamic data (Dorofeev, 2001).

Therefore, an “FA-index” may be defined for purposes of FA assessment:

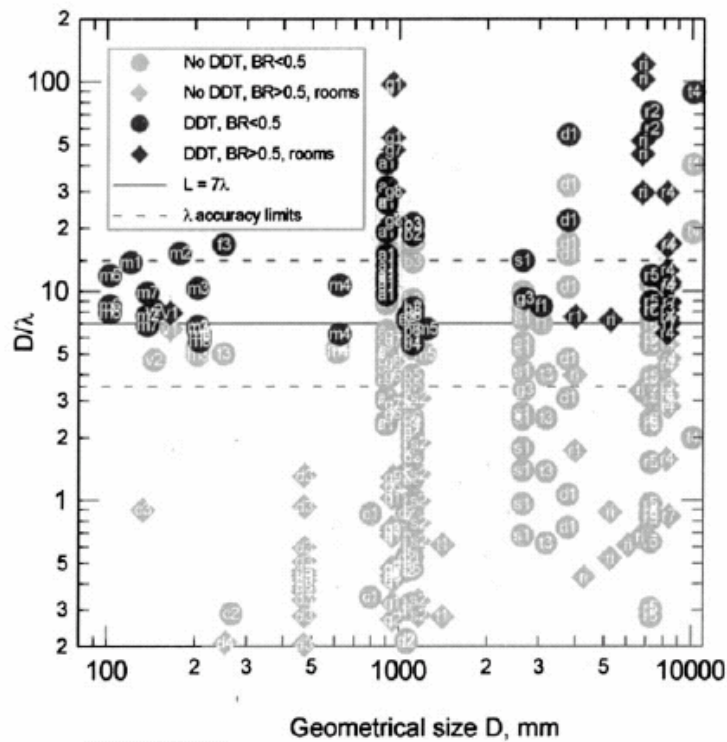
$$i_\sigma = \frac{\sigma}{\sigma^*} \quad (\text{Eq.2.4})$$

so that values of $i_\sigma \geq 1.0$ mean that FA is likely and unlikely if $i_\sigma < 1.0$. However, uncertainties in the model (8%) recommend reducing this threshold value to 0.92 (as been applied in the CPPC code).

2.4.3. Deflagration-to-detonation transition (DDT): the λ criterion

As an effect of the pressure wave, DDT occurs when a local reaction core is amplified and propagated from the reaction zone to the surroundings of the non perturbed mixture. A coherent coupling between the shock wave and the reaction zone must happen. From numerical simulations, Dorofeev et al. (1989) suggested that this process needs a minimum size of the reactive mixture. The subsequent experimental program performed in Germany, Russia, France and USA and the review of the available data in the literature have confirmed this result (Breitung, 2000). The analysis on facilities of different characteristic sizes have shown that the minimum mixture size for DDT must be above a certain value measured in units of detonation cell size, known as λ parameter (Figure 2.3). The minimum characteristic cloud size for DDT occurrence is $D \geq 7\lambda$:

Figure 2.3. Ratio between characteristic cloud size / detonation cell size of different detonable and non-detonable mixtures at several experimental sizes (Breitung, 2000).



A “DDT-index” for assessing the likelihood of DDT phenomena is therefore defined through:

$$i_{\lambda} = \frac{D}{7\lambda} \quad (\text{Eq.2.5})$$

so that DDT is possible when $i_{\lambda} \geq 1$ and, if $i_{\lambda} < 1$, DDT is discarded. Uncertainties in the model (43%) recommend reducing this threshold value to 0.57, which has been used at the CPPC code.

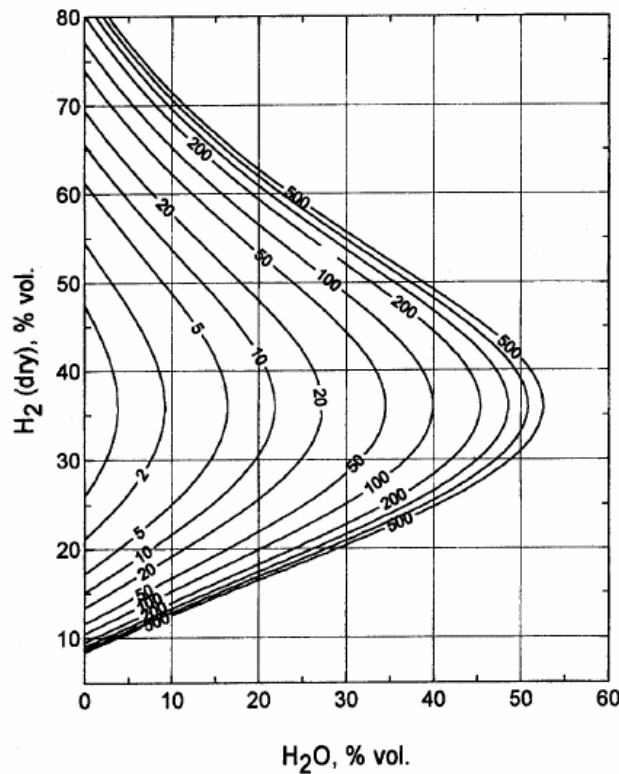
Characteristic size of the mixture is calculated in CPPC code under the hypothesis of homogeneous atmosphere, i.e. the mixture spreads throughout the full containment free volume (V), by following the basic expression recommended by (Breitung and Royl, 2000):

$$D = V^{1/3} \quad (\text{Eq.2.6})$$

The λ parameter is a property of the mixture, which depends on pressure, temperature and gas concentrations. A wide experimental database exists for this property, hence KI performed a minimum square fit of different analytical functions (CSNI, 2000) lying within the uncertainty limits of the experiments, which has been implemented in the CPPC code (Figure 2.4):

$$\log_{10}(\lambda) = f(X_{H_2, dry}, X_{H_2O}, T, p) \quad (\text{Eq.2.7})$$

Figure 2.4. Detonation cell size λ (cm) for H₂/air/steam mixtures at 375 K and 2 bar calculated with a experimental fitted functions, taken from (CSNI, 2000).



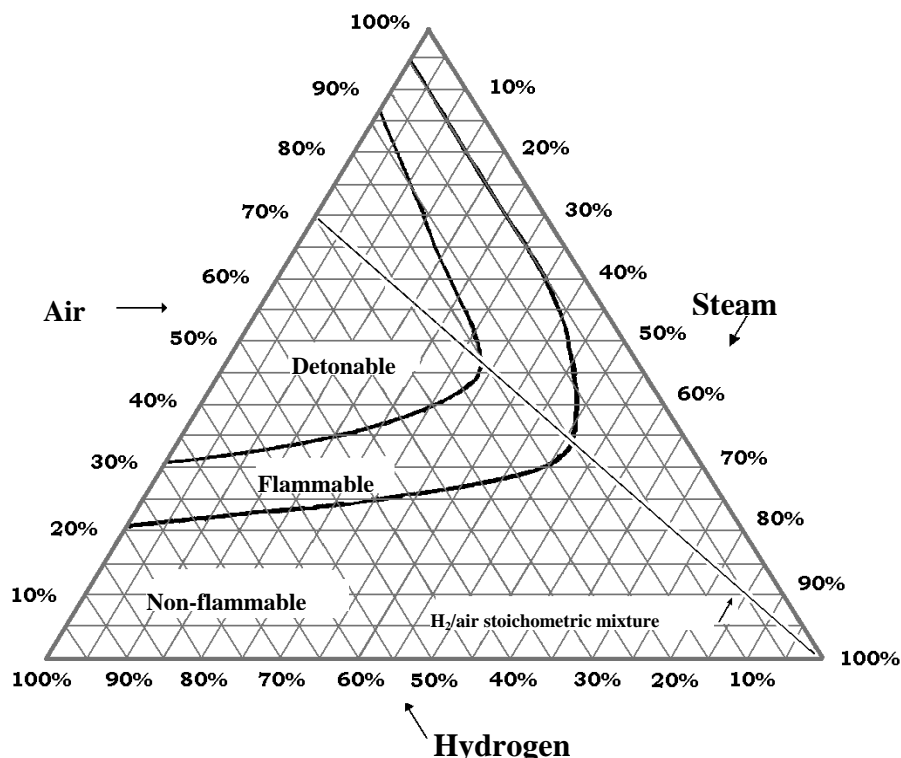
2.4.4. Direct detonation (DET)

The DET regime needs the mixture lying within the detonable limits, being the ignition energy high enough. The second effect is impossible to be evaluated with a simple code like CPPC, but a detonability region has been identified in the code, as from the Shapiro-Moffette diagram (Figure 2.5) by using linear functions of the hydrogen and steam molar fractions:

$$a_{\text{det}} X_{H_2O} + b_{\text{det}} X_{H_2} \leq c_{\text{det}} \quad d_{\text{det}} X_{H_2} \geq e_{\text{det}} \quad f_{\text{det}} X_{H_2O} \leq g_{\text{det}} \quad (\text{Eqs.2.8})$$

being a_{det} , b_{det} , c_{det} , d_{det} , e_{det} , f_{det} and g_{det} the coefficients fitting the Shapiro-Moffette diagram at 373 K (Martín-Valdepeñas, 2004b).

Figure 2.5. Shapiro-Moffette ternary diagram showing flammability and detonability limits for hydrogen/air/steam/mixtures at 373 K and 1 bar (Martín-Valdepeñas, 2004b).



2.5. Combustion completeness (CC)

The CC parameter indicates the fraction of the initial hydrogen within the flammable mixture that will actually be burnt. In the PSA level 2 studies, completeness during the global combustion is postulated, as based on the non well-mixed conditions of the mixture and the complex containment geometry. Some processes increasing the mixing and turbulence of the atmosphere (as containment spray actuation) enhance the combustion completeness.

Several empirical correlations have been developed for evaluating the CC parameter and are based on the H_2 , CO and steam molar fractions and the operating status of the water spraying. The CPPC code incorporates three sets of them, taken from the following references or codes:

- Pilch et al (1996),
- Murata et al (1997), taken from CONTAIN 2.0 and

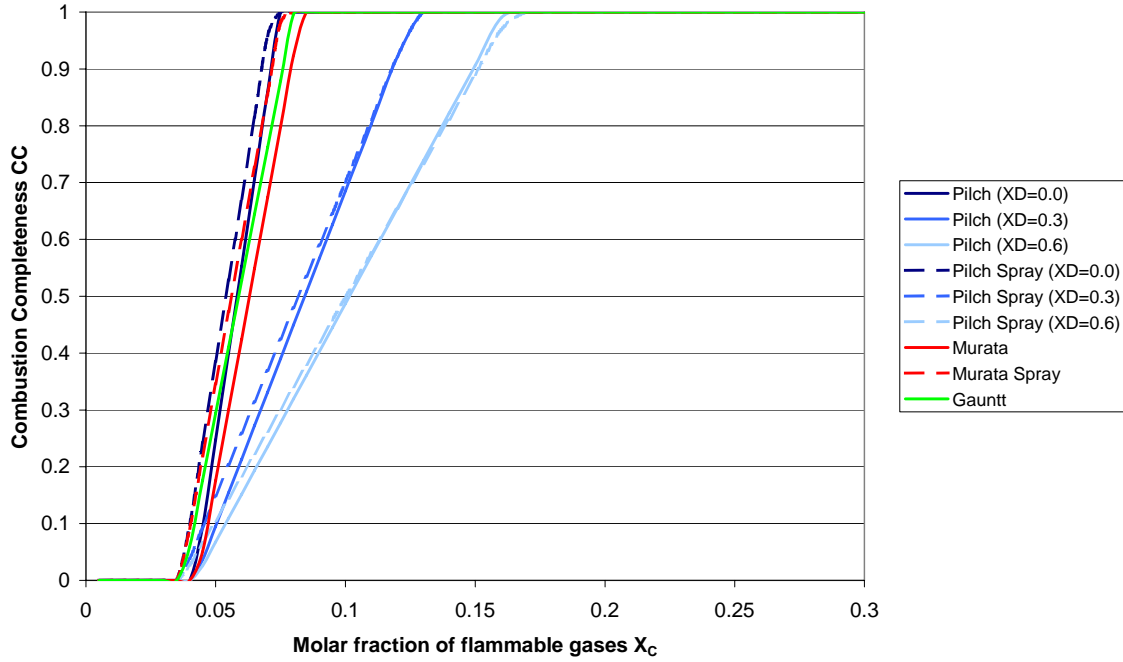
- HECTR 1.5, taken from MELCOR 1.8.4 (Gauntt ,1997).

CC could be generally expressed by:

$$CC = \text{Max}(\min((a_{CC} + b_{CC} X_{H_2} + c_{CC} X_{CO}) \exp(d_{CC} X_{H_2O} + e_{CC} X_{CO}), 1), 0) \quad (\text{Eq.2.9})$$

being a_{CC} , b_{CC} , c_{CC} , d_{CC} and e_{CC} experimental fitted coefficients. A comparison amongst these correlations is shown on Figure 2.6.

Figure 2.6. Comparison of the different CC models (with / without sprays) implemented on the CPPC code as function of the molar fraction of the flammable gases (X_C).



2.6. Containment static pressures

The pressure resulting from the H_2/CO combustion depends on the flammable cloud size, the mixture composition and the geometry. These parameters determine the possible combustion regime, as assessed by the criteria summarised above.

The pressure onto the containment structure due to a SD is the pressure peak developed during the combustion process (Breitung, 1997). This pressure is proportional to the amount of hydrogen burnt and its upper bound is the pressure assumed adiabatic isochoric complete combustion (AICC). The CPPC code calculates the p_{AICC} from an energy balance in an adiabatic, isochoric closed system under the hypothesis of complete combustion, as expressed in terms of the internal energy:

$$\sum_A (n_A c_{v,A})_b T_b^{AICC} = \sum_A (n_A c_{v,A})_u T_u + n_{H_2,q} q_{H_2} + n_{CO,q} q_{CO} \quad (\text{Eq.2.10})$$

being $c_{v,A}$ the specific heat at constant volume and n_A the number of moles of the species “A” in the mixture (O_2 , N_2 , H_2 , H_2O , CO and CO_2). T_u is the initial temperature (unburned gas mixture) and T_b^{AICC} is the resulting temperature of the burned gas by considering AICC combustion. Last two terms

in the RHS express the energy release by H₂ and CO reaction, considering the effect of completeness by reducing the moles of flammable gas with the CC calculated with (Eq.2.9).

Constant-volume specific heats are calculated from polynomial functions of temperature:

$$c_{vA} = \left(A_A + B_A T + C_A T^2 + D_A T^3 \right) \frac{R}{PM_A} - R \quad (\text{Eq.2.11})$$

being the constants A_A, B_A, C_A and D_A specific for each gas species, values taken from (Benson, 1977). The T_b^{AICC} is calculated from (Eq.2.10) through an iterative Newton-Raphson method.

The AICC pressure is calculated finally by considering a mixture of ideal gases in the equation:

$$p_b^{AICC} = p_u \left(\frac{T_b^{AICC}}{T_u} \right)^{\left(\frac{n_b}{n_u} \right)} \quad (\text{Eq.2.12})$$

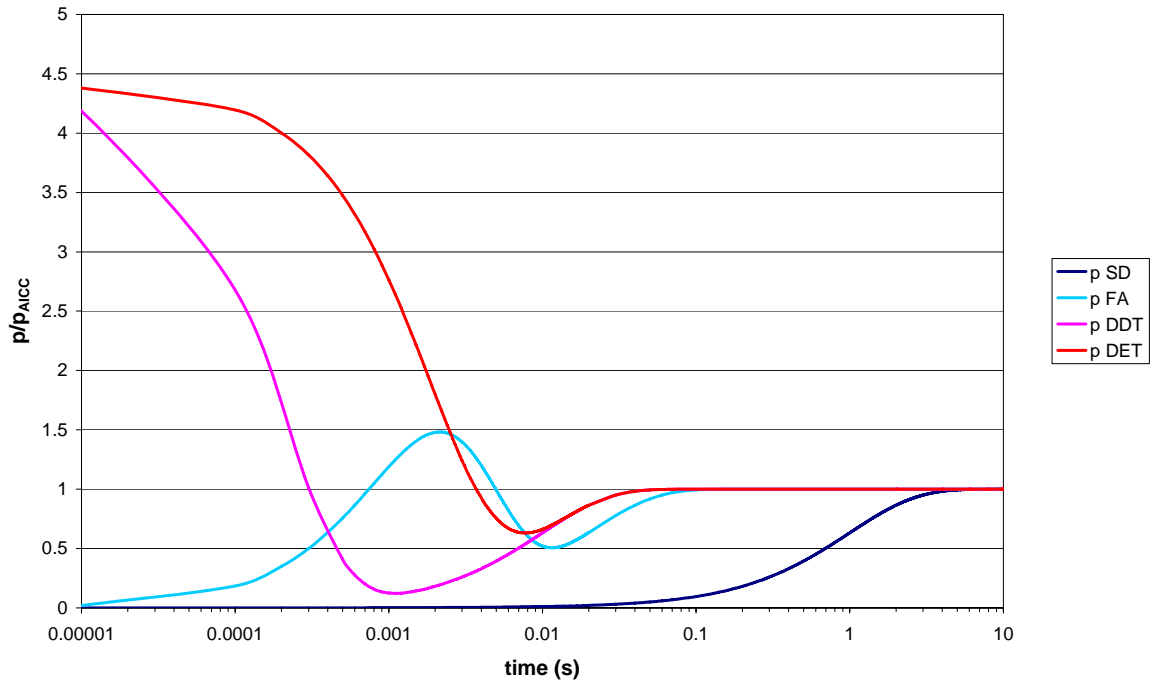
When combustion is turbulent both the flame front speed and the associated pressure rise are increased. If the conditions are adequate the FA or DDT could occur. In case of a DDT and during the onset of a detonation the maximum pressure developed is bounded by the Chapman-Jouguet pressure (p_{CJ}) and the maximum pressure peak comes from the reflected shock wave (p_{CJ-RF}) (Breitung, 1997).

These three theoretical pressure magnitudes, AICC, CJ and CJ-RF show the same dependence with the equivalence ratio, whereby Breitung (1997) proposed the following simple relationships to approach them in nuclear safety analysis.

$$p_{CJ} = 1.8(\pm 0.08)p_{AICC} \quad (\text{Eq.2.13})$$

$$p_{CJ-RF} = 4.1(\pm 0.3)p_{AICC} \quad (\text{Eq.2.14})$$

Figure 2.7. Typical shape of pressure loads at the different combustion regimes.



Nevertheless, the vulnerability of the containment structures does not depend only on the maximum pressure peak impinging over the wall, but on the time of structure-wave interaction and structural response. Breitung and Redlinger (1995b) consider that SD features a gradual increase of pressure, reaching the static pressure (bounded by the AICC) in time of seconds (Figure 2.7). In contrast, faster combustion regimes (FA, DDT and DET) show a rapid pressure rise, bounded by the C-J (direct for FA, reflected for the shock wave regimes DDT and DET) and followed by a sudden decrease down to the static steady pressure, bounded by the AICC. This process occurs in times of milliseconds (Figure 2.7).

Moreover, it is important to consider the structure response time, since comparison of both values permits to assess the containment deformation. Breitung and Redlinger (1995b) introduced a model based on the 1D simple harmonic oscillator to get an estimate, in a simple way, of the maximum deformations induced onto the containment structures by the pressure loads developed under the different combustion regimes. The effective static load equivalent to the maximum deformation (an effective value of pressure, p_{eff}) is calculated accordingly. This effective pressure is to be compared to the fragility curve for the assessment of the containment integrity.

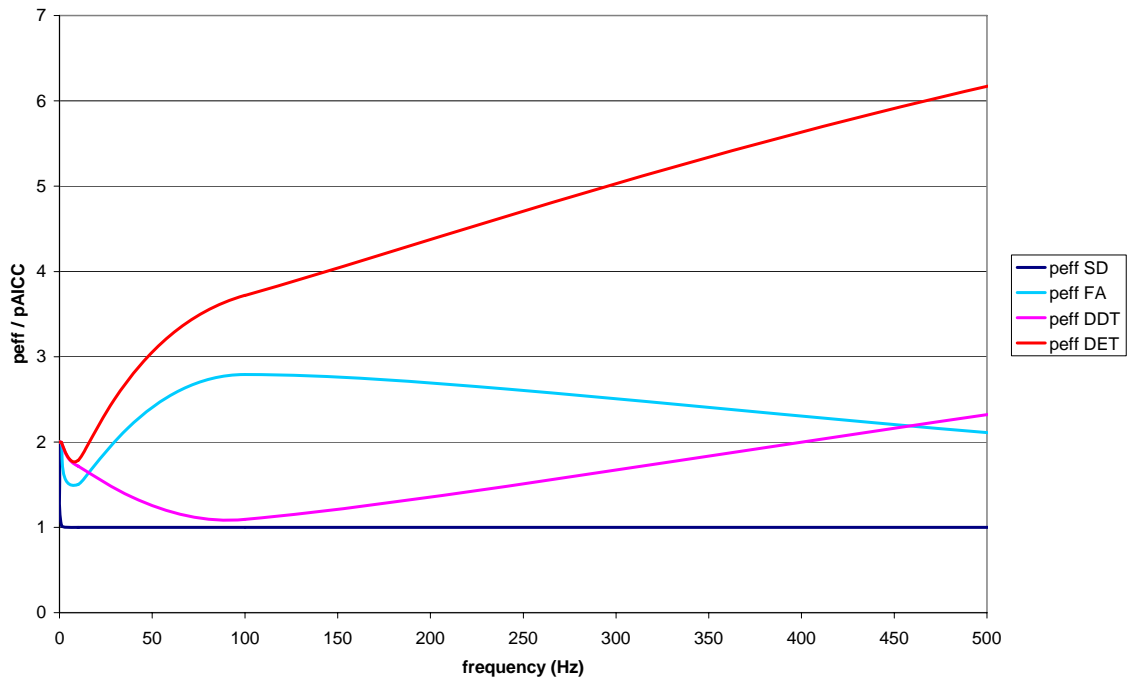
This model has been implemented in the CPPC code. The 1D simple harmonic oscillator equation has been solved for the different pressure loads $p_i(t)$:

$$y'' + (2\pi f)^2 y = \frac{p_i(t)}{m} \quad (\text{Eq.2.15})$$

being y the oscillator (structure) elongation, f the natural frequency of the structure and m its mass per unit of surface area. The code solves this equation and identifies the maximum elongation y_{max} . Then the effective static pressure load is calculated by:

$$p_{eff} = (2\pi f)^2 m y_{max} \quad (\text{Eq.2.16})$$

Figure 2.8. Effective static pressure normalised at the AICC vs typical frequency of the containment structures as calculated with the CPPC code.



On Figure 2.8 the evolution of this effective pressure is depicted within the frequency range typical of the containment structures: ~5 to 500 Hz as indicated by Breitung and Redlinger (1995b). This figure has been calculated with the CPPC code for a typical concrete structure 1 m-thick, and shows that the SD effective pressure is independent of the frequency at the containment typical frequencies. This pressure is equal to the AICC because the SD develops a static pressure. However, dynamic effects are observed in the other combustion regimes (FA, DDT and DET), where the effective pressure depends on the combustion and the structure response modes, and ranges from the AICC pressure to 6 times this value.

3. Validation and verification process

This section describes some of the most relevant aspects of the validation and verification procedures for the CPPC code. CPPC results have been compared with the results obtained with other codes for AICC calculations in case of slow deflagrations. Results are very satisfactory, because the differences in the pressure increase range in the 1%.

3.1 Validation with results by Breitung and Redlinger

The AICC pressure rise was checked with the outcomes obtained by Breitung and Redlinger (1995a). Table 3.1 shows the results of the CPPC calculations as well as a comparison with those obtained by Breitung and Redlinger.

Table 3.1. Comparison between Breitung and Redlinger (1995a) results and CPPC calculations for AICC pressure in different H₂-steam-air mixtures.

X _{H2} (% vol)	X _{H2O} (% vol)	T _u (*) (K)	P _u (*) (bar)	AICC pressure (bar)		Deviation (%)
				Breitung	CPPC	
15.0	30	362	2.26	9.953	10.03	-0.8
20.0	40	380	3.26	14.482	14.4	0.6
20.0	30	366	2.58	13.294	13.5	-1.5
15.0	15	335	1.62	7.487	7.95	-1.3
20.0	0	293	1.27	8.618	8.82	-2.3
29.5	0	293	1.44	11.875	12.77	-7.5
30.0	15	342	2.12	13.316	13.36	-0.3
25.0	30	368	2.84	14.282	14.24	0.3

(*) Unburnt gas conditions prior to combustion.

Relative errors lie around 1%, except for dry mixtures where deviations are larger, although less than 10%. In principle, these results are considered as acceptable.

3.2 CPPC application to the analysis of steam deinertisation within a PWR containment

The objective of this section is approaching the pressure onto the containment external structures developed by the combustion of hydrogen and carbon monoxide generated during a severe accident in PWR containments. Particularly, the analysis aimed at exploring the effects of deinertisation of the containment atmosphere by the late actuation of the containment heat removal system (CHR) during the ex-vessel phase of a postulated severe accident within a typical PWR containment. The analysis is based on the application of the MELCOR 1.8.5 code (Gauntt, 1997).

With the aim of contrasting the main assumptions in the BUR gas combustion module in MELCOR with those of the adiabatic-isochoric complete combustion (AICC), a comparison exercise is performed between the results of the MELCOR and the CPPC codes for selected severe accident

scenarios involving combustible gas generation during in-vessel and ex-vessel phases, and by the actuation of the containment heat removal system (CHR) promoting atmosphere deinertisation.

3.2.1 Calculation models and assumptions

Accident analysis refers to the evolution of a prototypical SBO sequence yielding a SB-LOCA with in-vessel core damage within a prototypical PWR. Time of vessel failure is predicted to happen 4 hours after the initiating event ($t=14400$ s). Released masses of materials in the in-vessel phase are put into the containment as mass and enthalpy sources obtained from a previous analysis for a scaled S3-TB' sequence (Martín-Fuertes, 1995). Released mass of hydrogen (304 kg) corresponds to the oxidation of 40% of the in-core Zr, and liquid water (100000 kg) and steam (80000 kg) are enough to provide steam-inerted conditions of the containment atmosphere at the time of vessel failure.

Further evolution after vessel failure has been simulated by assuming melt material pouring to cavity (100% of UO_2 , 60% of metallic Zr, 40% of oxidised Zr, 8000 kg of SS), CHR activation at different times and the MCCI gas release into either wet or dry cavity. Accident simulation is extended to the first 24 h. Mass sources during the ex-vessel phase will be simulated by applying the CAV module in MELCOR and by exploring the possibility of cavity flood during the accident. Two kind of scenarios are distinguished thereby: 'dry' and 'wet'. It is worthwhile noting that the situations of dry or wet cavity do not influence the total amounts of H_2 and CO generated. They are practically identical (188 kg of H_2 and 3750 kg of CO), except for the short delay in their production under wet cavity conditions.

Under these conditions, atmosphere is expected to deinertise and eventually burn shortly after the start of the CHR activation. Values of containment pressure increased by the effect of a (assumed unique) combustion will be calculated with the CPPC code and with the BUR package in MELCOR, and code results will be compared.

3.2.2 Analysis with MELCOR and CPPC codes

For analysing the effect on the maximum containment pressure caused by the atmosphere deinertisation by the CHR systems (water spraying and fan coolers) actuation. Times for CHR activation during the sequence may be selected by criteria of power recovery or accident management procedures. According to this, two characteristic starting times of these systems have been defined:

- T0: scenarios with CHR activation coincident with vessel failure (time=14400 s).
- T1: scenarios with CHR activation coincident with the maximum of the σ parameter (23700 s for 'dry' scenarios, 21100 s for 'wet' ones).

T0 is related to containment atmosphere combustions with the maximum combustible gas amount (only hydrogen) released during the in-vessel phase. On the other hand, T1 is related to the maximum combustible gas (H_2 and CO) amounts expectable during the whole accident.

As long as the objective of the analysis is the assessment of the risk of containment failure due to atmosphere combustion caused by deinertisation by CHR actuation, it will be assumed that gas combustions are unique and the most complete during the accident (namely, all of the combustible gas able to be burnt is consumed at the same time). In the MELCOR analysis, combustion completeness is determined by the code default model. Combustion is assumed to start at any room reaching the flammability limits, hence assuming that effective ignition sources are located anywhere. It must be mentioned that the combustion regime considered in current version of the BUR package is that of deflagration with linear progression.

On the other hand, containment atmosphere deinertisation by CHR actuation is calculated by the code depending on the containment atmosphere conditions and the operating capacity of the CHR. Concerning this last issue, the following variations are also considered:

- ESF: Nominal capacity of the CHR systems (containment spray and fan-cooling units) under accident conditions.
- FCL: Full-capacity of the fan-cooling system (no containment spray).
- SPR: Full capacity of the containment spraying system (no fan-cooling units).

The maximum pressure obtained by analysis with the MELCOR code will be compared to the value obtained by the CPPC code. MELCOR results for gas burns occurred in T0 scenarios are analysed on next table:

Table 3.2a. Summary of MELCOR results for H₂ combustions in T0 scenarios.

Scenario	Time (s)	Duration (s)	H ₂ (CO) mass burnt (kg)	p _{max} (bar)
dryT0-ESF	18813	70	51 (229)	1.69
dryT0-FCL	18609	58	80 (331)	1.96
dryT0-SPR	20719	31	120 (1175)	2.23
wetT0-ESF	22497	57	424 (3145)	5.11
wetT0-FCL	22263	57	424 (3149)	5.11
wetT0-SPR	19328	17	374 (1914)	4.45

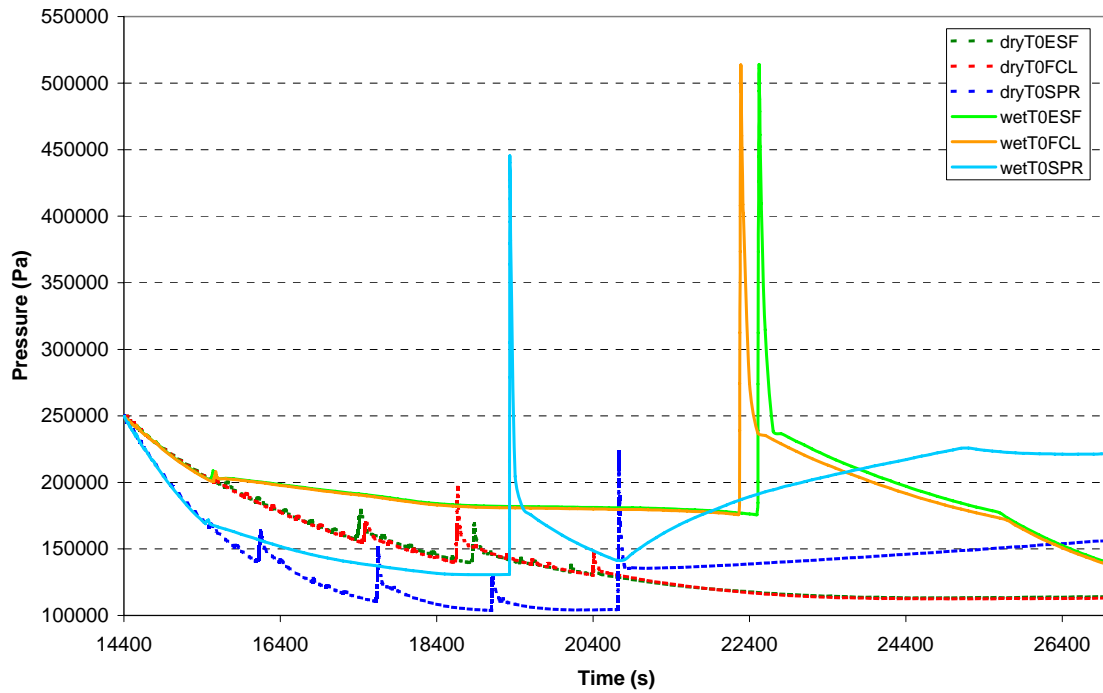
On the other hand, previous results may be compared to those obtained by application of the CPPC code (where the “complete combustion” option has been applied):

Table 3.2b. Summary of CPPC results for H₂ combustions in T0 scenarios.

Scenario	p _{AICC} (bar)	p _{CJ} (bar)	p _{CJrefl} (bar)	p _{eff} (bar)	FA indx	DDT indx	Regime
dryT0-ESF	4.110	7.726	18.082	4.109	0.719	0.000	SD
dryT0-FCL	4.106	7.720	18.068	4.106	0.720	0.000	SD
dryT0-SPR	3.996	7.512	17.581	3.995	0.848	0.015	SD
wetT0-ESF	6.483	12.188	28.525	10.300	0.927	0.015	FA
wetT0-FCL	6.495	12.210	28.576	10.318	0.929	0.016	FA
wetT0-SPR	5.175	9.728	22.768	5.174	0.912	0.017	SD

It is evidenced that dry-cavity scenarios (‘dryT0’) feature combustions affecting limited regions of the containment and therefore involve only a fraction (below 25%) of the total combustible gas amount available. Maximum pressures therefore lie much below p_{AICC}. On the other hand, in wet cavity scenarios (‘wetT0’), a longer time is required for the CHR to deinertise the containment atmosphere. More energetic and complete combustions (80% to 90%) are expected and maximum pressures reach thereby values close to the p_{AICC}. In scenarios where FA is predicted by CPPC, values of the effective pressure p_{eff} rise up to near 2×p_{AICC} and thereby closer to the containment failure pressure. Because of the larger full-capacity of the water spraying system, earlier combustions are predicted in the SPR cases. The apparently late burn during the ‘dryT0SPR’ scenario is not in disagreement with this, since it is not the first and unique combustion, but the larger and last of a early-starting series (see Figure 3.1) and thus selected on Table 3.2a as being the most AICC-like. Results obtained through the application of the MELCOR code for these scenarios are illustrated next on Figure 3.1, where pressure evolution in the containment is represented.

Figure 3.1. Containment pressure evolution predicted by MELCOR during T0 scenarios.



Analogously, results corresponding to CHR activation coincident with the maximum value of the parameter σ (time=T1) are introduced on next Table 3.3(a and b) and Figure 3.2. MELCOR and CPPC results for these situations are summarised next:

Table 3.3a. Summary of MELCOR results for H₂ combustions in T1 scenarios.

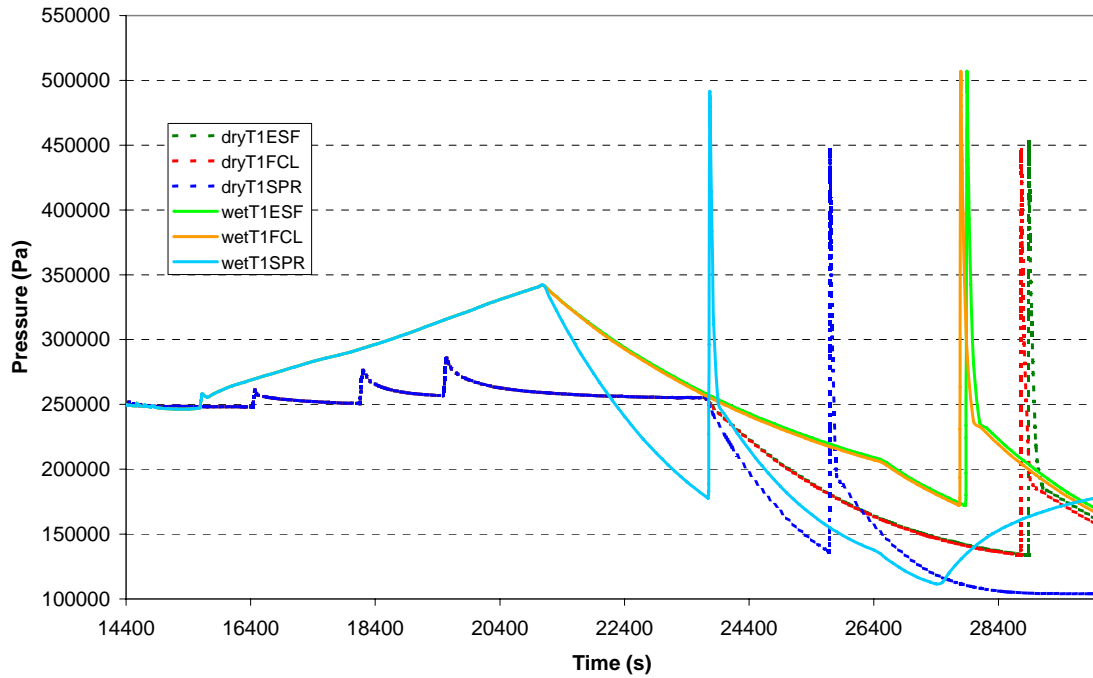
Scenario	Time (s)	Duration (s)	H ₂ (CO) mass burnt (kg)	p _{max} (bar)
dryT1-ESF	28882	46	364 (2848)	4.53
dryT1-FCL	28754	58	361 (2644)	4.46
dryT1-SPR	25685	44	360 (2635)	4.46
wetT1-ESF	27869	88	420 (3138)	5.07
wetT1-FCL	27771	86	422 (3155)	5.07
wetT1-SPR	23741	89	419 (3129)	4.92

Table 3.3b. Summary of CPPC results for H₂ combustions in T1 scenarios.

Scenario	p _{AICC} (bar)	p _{CJ} (bar)	p _{CJrefl} (bar)	p _{eff} (bar)	FA indx	DDT indx	Regime
dryT1-ESF	5.322	10.005	23.416	8.455	0.952	0.033	FA
dryT1-FCL	5.332	10.024	23.461	8.471	0.948	0.030	FA
dryT1-SPR	5.378	10.110	23.662	8.544	0.945	0.030	FA
wetT1-ESF	6.374	11.983	28.045	10.127	0.928	0.014	FA
wetT1-FCL	6.375	11.984	28.048	10.128	0.928	0.014	FA
wetT1-SPR	6.453	12.131	28.391	6.452	0.916	0.011	SD

Most of the T1 scenarios are characterised by the onset of a unique combustion by CHR actuation, except for very small burns in ‘dryT1SPR’ shown on Figure 3.2. Since the whole amount of combustible gases to be released is already present in the containment atmosphere, all of the cases are expected to feature pressure values similar to one another and to the AICC pressure (like the ‘wetT0’ scenarios on previous paragraphs), being the CPPC calculations for p_{eff} much above the p_{AICC} when FA is predicted. Additionally, earlier combustions are observed for the SPR cases, because of their higher deinerting capacities, thereby showing the highest maximum pressure values in this case.

Figure 3.2. Containment pressure evolution predicted by MELCOR during T1 scenarios.



From the analysis above, the effective pressure p_{eff} may rise up to values close to the containment failure pressure when FA is predicted. Nevertheless, it must be reminded that, because of the simplifying assumptions considered in the CPPC code -combustion is complete and unique, the amplitude of pressure profiles ranges between the extreme theoretical values p_{CJ} and p_{AICC} (Figure 2.7)- these predictions should rather be interpreted as an upper bound of the actual loads onto the containment. Consequently, more detailed analysis are recommended for these situations.

4. PLANT APPLICATIONS

A program to apply CPPC to plant calculations is currently in progress in CSN. The first stage is the calculation of the containment failure probability for a large-dry PWR containment in case of H_2 burn during the in-vessel phase of a severe accident. CSN methodology to calculate the containment failure probability due to hydrogen combustion prior to and at vessel breach is as follows:

- Obtain the baseline containment pressure prior to any hydrogen combustion (prior to, and after vessel breach) using the plant-specific MELCOR calculations.
- Obtain the hydrogen mass in the containment before the combustion (see below for further explanations). It is considered that H_2 is uniformly distributed inside the containment.
- Calculate the containment pressurization due to an adiabatic, isochoric, combustion model, assuming that the degree of combustion completeness is a function of the pre-burn hydrogen concentration, as correlated by experimental data. The CPPC code would help in this step.
- Overlap the containment pressure distribution with the plant specific containment fragility curve to arrive at the containment failure probability.

Table 4.1. Probability density functions for Zr oxidation in PWR high pressure severe accident scenarios.

Probability	Fraction of Zr oxidized	Proposed Zr oxidation fraction for scenarios involving reflooding
0	0.0 - 0.15	0.0 – 0.35

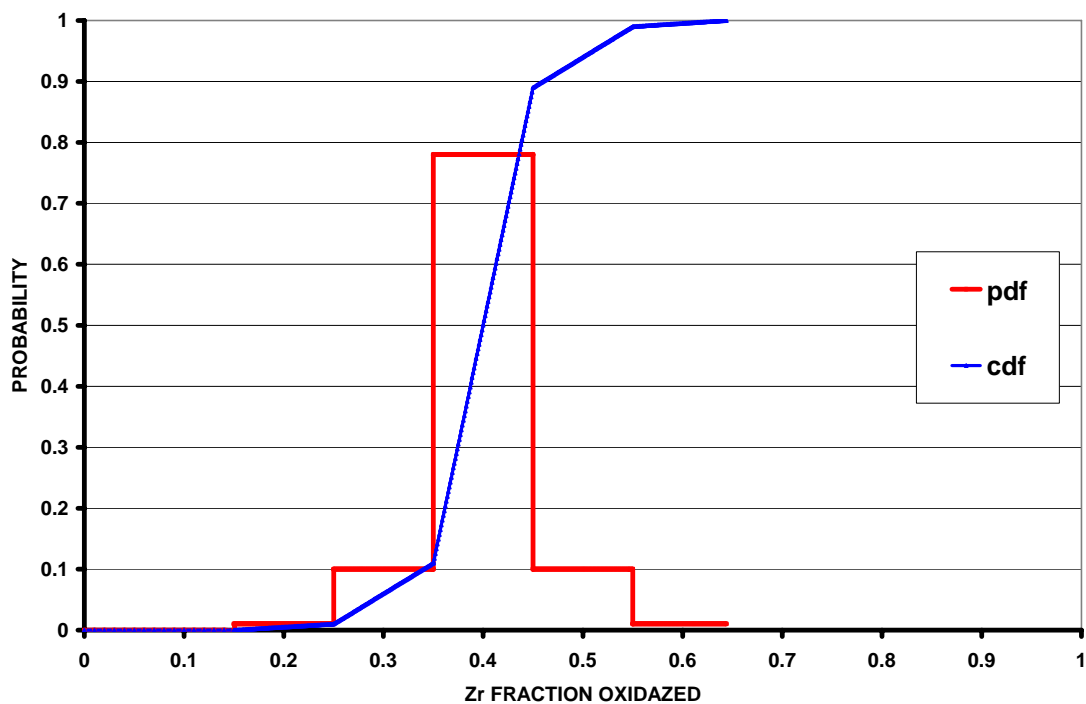
0.01	0.15-0.25	0.35 – 0.45
0.1	0.25-0.35	0.45 – 0.55
0.78	0.35-0.45	0.55 – 0.65
0.1	0.45-0.55	0.65 – 0.75
0.01	0.55-0.644	0.75 – 0.844
0	0.644-1	0.844 – 1

Hydrogen mass within the containment before its burn may be entered from the probability density function (pdf) considered by the NRC for the resolution of the direct containment heating issue, (Pilch, 1994). Table 4.1 provides this pdf and Figure 4.1 depicts the pdf and cumulative distribution function (cdf) for this random variable in the case of no reflooding.

Note that these values are conservative as they are obtained from accidents involving high pressure in the RCS. In addition, most of the severe accident sequences in Spanish PWR plants evolve with low pressure in the RCS.

As shown on Table 4.1, severe accident scenarios to be managed by core reflooding have been considered in this methodology. Based on the results from (Kuan, 1994) it was considered an absolute increase of 20% for Zr oxidation in these scenarios.

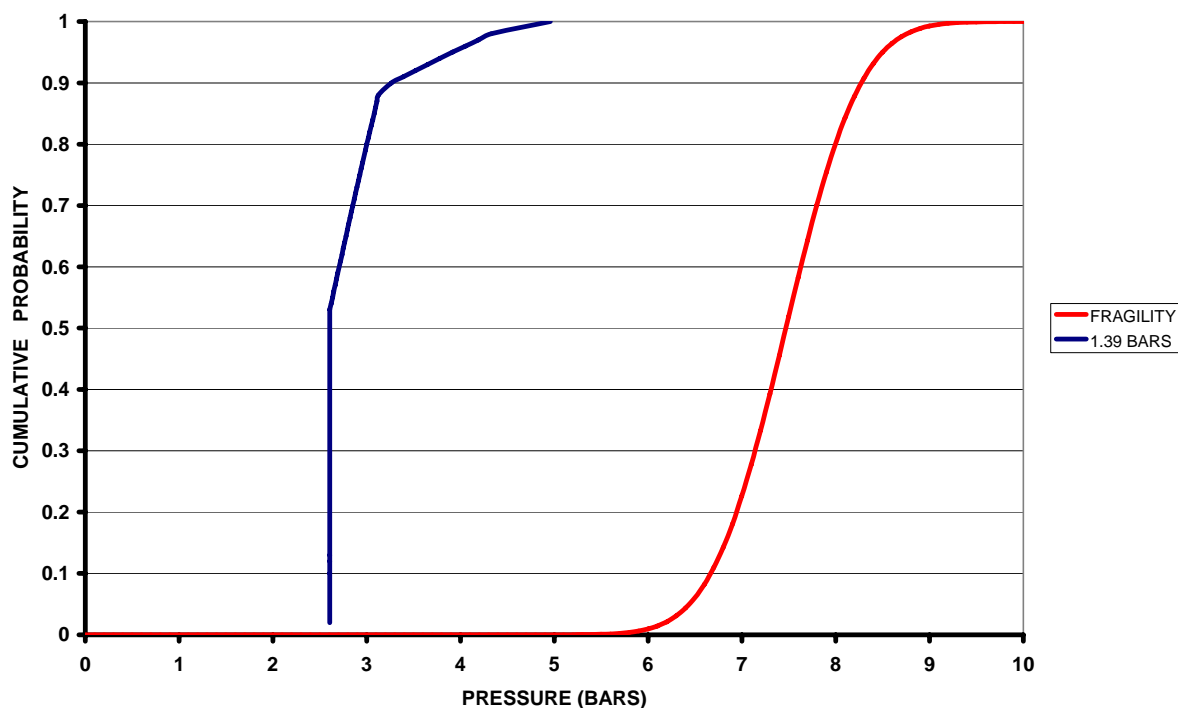
Figure 4.1. pdf and cdf for Zr oxidized fraction in PWR (no reflooding case).



The results obtained show that the containment failure probability is negligible in case of no reflooded scenarios. Figure 4.2 shows the cdf's for both the containment pressure rise by hydrogen combustion and the containment fragility curve for a typical Spanish PWR in case of no reflooding. Nevertheless, for reflooding scenarios, the containment failure probability would increase significantly, since in the upper edge of the Zr oxidation fraction distribution, the hydrogen would burn as a fast deflagration with the corresponding pressure increase by the hydrogen combustion. Safety significance of this phenomenon is under study.

Future applications are planned, including the calculation of the containment failure probability for the ex-vessel phase and analyses of local hydrogen accumulations in containments.

Figure 4.2. cdf's for containment loads from hydrogen burn and containment fragility for a typical Spanish PWR. No reflooding.



5. References

- Benson R S, "Advanced Engineering Thermodynamics", Pergamon Press, Oxford, 1977.
- Breitung W, Redlinger R, "Containment Pressure Loads from Hydrogen Combustion in Unmitigated Severe Accidents". IKET-FzK, Nuclear Technology 111, 395-419, 1995a.
- Breitung W, Redlinger R, "A Model for Structural Response to Hydrogen Combustion Loads in Severe Accidents". IKET-FzK, Nuclear Technology 111, 420 – 425, 1995b.
- Breitung W, "The Analysis of Hydrogen Behaviour in Severe Accidents", EURO COURSE-97: Analysis of Severe Accidents in Light Water Reactors, F²T², EC- Nuclear Fission Safety Programme, Madrid (Spain), 13-17 October 1997.
- Breitung W, Royl P, "Procedure and Tools for Deterministic Analysis and Control of Hydrogen Behaviour in Severe Accidents", IKET-FzK, Nuclear Engineering and Design 202, 249-268, 2000.
- CAB, "TABAGUA: Program for Light Water Properties", Centro Atómico de Bariloche, 1988.
- CSNI Group of Experts, State of the Art Report "Flame Acceleration and Deflagration to Detonation Transition in Nuclear Safety", NEA/CSNI/R(2000)7, 2000.
- Dorofeev S B, Kotchourko A S, Chaivanob B B, "Detonation Onset Conditions in Spatially Non-Uniform Combustible Mixtures". Proceedings of the 6th International Symposium on Loss Prevention and Safety Promotion in the Process Industries 4, 221, Oslo, 1989.

Dorofeev S B, Kuznetsov M S, Alekseev V I, Efimenko A A, Breitung W, “Evaluation of Limits for Effective Flame Acceleration in Hydrogen Mixtures”. RRC-KI/FzK. Journal of Loss Prevention in the Process Industries 14, 583-589, 2001.

Gauntt R O et al., “MELCOR Computer Code Manuals”, Version 1.8.4, NUREG/CR-6119, Vols 1 and 2, Rev 1, SAND97-2398, July 1997.

Khatib-Rahbar et al, “A Regulatory Evaluation of the CN Vandellós Probabilistic Safety Analysis (Level-2)”. ERI/CSN 97-801. December 1997.

Khatib-Rahbar et al, “A Regulatory Evaluation of the CN Almaraz Probabilistic Safety Analysis (Level-2)”. ERI/CSN 98-801. September 1998.

Khatib-Rahbar et al, “A Regulatory Evaluation of the CN Ascó Probabilistic Safety Analysis (Level-2)” ERI/CSN 00-801. June 2000.

Khatib-Rahbar et al, “A Regulatory Evaluation of the CN Trillo Probabilistic Safety Analysis (Level-2)”. ERI/CSN 01-801. July 2001.

Khatib-Rahbar et al, “A Regulatory Probabilistic Safety Analysis (Level-2) of the José Cabrera Nuclear Power Plant”. ERI/CSN 02-801. August 2002.

Kuan, “Implications for Accident Management of Adding Water to a Degrading Reactor Core”. NUREG/CR - 6158. February 1994.

Kumar RK, “Flammability Limits of Hydrogen-Oxygen-Diluent Mixtures”, Journal of Fire Science 3 (4), 245-262, 1985.

Kuznetsov M, Dorofeev S, Breitung W, “Analysis of the new experimental data on flammability and flame acceleration limits at low pressures and application to the LOVA sequence”, IKET-FzK, EFDA, Task TW3-TSS-SEA3.5, Karlsruhe, 2003.

Marshal B W, “Flammability Limits and Combustion Characteristics of Hydrogen-Air-Steam at Intermediate Scale”. SAND86-0579C, 1986.

Martín-Fuertes F, Fernández J A, Meléndez E, “MELCOR 1.8.2 Calculations of Two Blackout-Type Accidents (TMLB’ and S3-TB’). A Partial Comparison with SCDAP/RELAP5”. Chair of Nuclear Technology (UPM)-CSN. CTN-06/95. Madrid 1995.

Martín-Valdepeñas J M, Jiménez M A, Martín-Fuertes F, “Desarrollo de un código para el Cálculo Probabilista de la Presión por Combustión de H₂ y CO en contención durante un accidente severo para su aplicación a estudios de APS Nivel 2 (CPPC)”. Chair of Nuclear Technology (UPM)-CSN. CTN-07/04. Madrid 2004a.

Martín-Valdepeñas J M, “Modelos Numéricos Acoplados a un Código Fluidodinámico para el Análisis del Riesgo de Combustión de Hidrógeno en Contenciones”, PhD Thesis, UPM, Madrid 2004b.

Murata KK et al., “Code Manual for CONTAIN 2.0: A Computer Code for Nuclear Reactor Containment Analysis”. NUREG/CR-6533, 1997.

Pilch M M, et al, “The Probability of Containment Failure by Direct Containment Heating in Zion”. NUREG/CR - 6075. July 1994.

Pilch M M, et al., “Resolution of the Direct Containment Heating Issue for all Westinghouse Plants with Large Dry Containments or Subatmospheric Containments”. NUREG/CR-6338, 1996.

Stamps D W, Berman M, “High-Temperature Hydrogen Combustion in Reactor Safety Applications”, Nuclear Science Engineering 109, 39, 1991.